An Improved Network Modeling of Slot-Coupled Microstrip Lines

Jeong Phill Kim, *Member, IEEE,* and Wee Sang Park, *Member, IEEE*

***Abstract*— This paper proposes an analytical method for slot-coupled microstrip lines with a view to developing an improved network model, which reflects the effects of inclination angles and offset distances. The network model consists of two ideal transformers and an extended slotline. The turn ratios are calculated by applying the reciprocity theorem with the spectral-domain immittance approach. The corresponding network models for several different configurations of these slot-coupled microstrip lines are then explored and shown to yield accurate scattering parameters.**

***Index Terms*— Circuit model, coupled microstrip lines, reciprocity theorem, spectral-domain analysis, slot.**

I. Introduction

As MICROWAVE circuits have been progressing toward monolithic microwave integrated circuits (MMIC's), coupling devices to interconnect high-density multilayer microstrip assemblies (e.g., a slot-coupled microstrip/microstrip transition, an out-of-phase power divider, a directional coupler, and the feed network of an active phased-array antenna) are playing an increasingly important role. Slot-coupled microstrip lines, created by cutting a narrow slot on the common ground plane of two back-to-back microstrip lines, are a promising candidate for this purpose.

The theory of coupling through small holes [1] and an approximate method based on a quasi-TEM mode [2] have both been used to analyze slot-coupled microstrip lines. Recently, full-wave analyses based on the reciprocity theorem with spectral-domain analysis [3]–[8], the mixed potential integral equation [9], and the transmission-line matrix (TLM) method [10] have also been successfully applied. However, these rigorous approaches do not provide conceptual insight into the coupling circuit, and require extensive numerical computations. Some network models have been proposed and applied to the analysis and design of slot-coupled microstrip circuits with an orthogonal and centered slot [5], [11], [12]. However, these models do not accommodate the effects of various structure parameters pertaining to slot-coupled microstrip lines.

This paper presents an analysis method of slot-coupled microstrip lines with a view to developing an improved equivalent-network model, which can tolerate the effects of various structure parameters, including inclination angles and offset distances. The proposed equivalent network consists of ideal transformers and slotline stubs. The turn ratios of the transformers are calculated by invoking the reciprocity theorem [13] with the spectral-domain immittance approach [14]. The scattering parameters are determined from the equivalent circuit by using the general-network theory [15]. The resulting model is then applied to several versions of the slot-coupled microstrip lines with different slot lengths, inclination angles, and offset distances. Finally, the computed scattering parameters of the proposed model are compared with the measured as well as the computed results from previous theories and the rigorous solution.

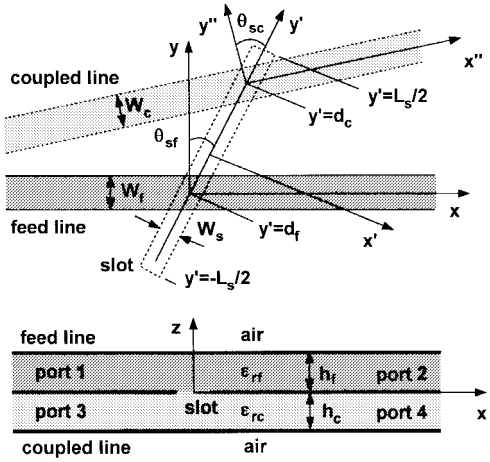

Fig. 1. Top and side views of the slot-coupled microstrip lines.

Section II defines the nature of slot-coupled microstrip lines and describes the analysis method based on the reciprocity theorem. In Section III and the Appendix, the expressions for the equivalent-circuit parameters are formulated using the finite Fourier transform and the spectral-domain immittance approach. Six different versions of slot-coupled microstrip lines are analyzed in Section IV, and their scattering parameters are compared. Conclusions are given in Section V.

II. Analysis Method

Fig. 1 is a scheme of the slot-coupled microstrip lines. The top microstrip line is a feed line, and the bottom one is a coupled line. The substrate of the feed line has a dielectric constant of $\epsilon_{\rm rf}$ and a thickness of h_f. The width of the feed line is W_f. The substrate of the coupled line has a dielectric constant of $\epsilon_{\rm rc}$ and a thickness of h_c. The width of the coupled

Manuscript received May 26, 1997; revised November 5, 1997.

J. P. Kim is with the Research and Development Center, LG Precision Company Ltd., Yongin, Kyunggi-Do 449-910, Korea.

W. S. Park is with the Department of Electronic and Electrical Engineering, Pohang University of Science and Technology, Pohang, Kyungbuk 790-784, Korea.

Publisher Item Identifier S 0018-9480(98)02738-0.

line is W_c. L_s and W_s denote the length and width of the coupling slot. The slot is arbitrarily inclined to the feed and coupled lines at the angles $\theta_{\rm sf}$ and $\theta_{\rm sc}$, respectively. d_f and d_c denote the offset displacements of the feed and coupled lines with respect to the center of the slot.

An incident field is first launched from $x = -\infty$ into port 1. The incident field exists only on the feed line, while the scattered field generated by the slot on the ground plane affects both the feed and coupled lines. Since the total field can be expressed as the sum of the incident and scattered fields, the total electromagnetic field at the ith port $\overline{E}_i$ and $\overline{H}_i$ $(i = 1 \sim 4)$ is stated as

$$\overline{E}_i = \begin{cases} \overline{e}_{\rm inc} + \Gamma_i \overline{e}_i, & \text{for } i = 1,2 \\ \Gamma_i \overline{e}_i, & \text{for } i = 3,4 \end{cases} \tag{1}$$

$$\overline{H}_i = \begin{cases} \overline{h}_{\rm inc} + \Gamma_i \overline{h}_i, & \text{for } i = 1,2 \\ \Gamma_i \overline{h}_i, & \text{for } i = 3,4 \end{cases} \tag{2}$$

where $\overline{e}_{\rm inc}$ and $\overline{e}_i$ are given as

$$\overline{e}_{\rm inc} = \overline{e}_f^{+} e^{-j\beta_f x} \tag{3}$$

$$\overline{e}_i = \begin{cases} \overline{e}_f^{-} e^{+j\beta_f x}, & \text{for } i = 1 \\ \overline{e}_f^{+} e^{-j\beta_f x}, & \text{for } i = 2 \\ \overline{e}_c^{-} e^{+j\beta_c x''}, & \text{for } i = 3 \\ \overline{e}_c^{+} e^{-j\beta_c x''}, & \text{for } i = 4. \end{cases} \tag{4}$$

The expressions of $\overline{h}_{\rm inc}$ and $\overline{h}_i$ can be obtained when $\overline{e}$ is replaced by $\overline{h}$ in (3) and (4). The subscripts f and c in (3) and (4) stand for the feed and coupled lines, respectively. Hereafter, this convention for the subscript will be used. β_f and β_c are the propagation constants of the corresponding microstrip lines. The field eigenvectors of the feed line $\overline{e}_f^{+}$ and $\overline{h}_f^{+}$ in (3) and (4) are normalized such that

$$\iint_{S_f} (\overline{e}_f^{+} \times \overline{h}_f^{+}) \cdot \hat{x}\, dy\, dz = 1 \tag{5}$$

where S_f is the cross section of the feed line. Three other pairs of field eigenvectors—$\overline{e}_f^{-}$ and $\overline{h}_f^{-}$, $\overline{e}_c^{+}$, and $\overline{h}_c^{+}$, and $\overline{e}_c^{-}$ and $\overline{h}_c^{-}$—are similarly normalized. Γ_i in (1) and (2) represents a quantity related to the scattered field due to the induced voltage across the slot.

Invoking the reciprocity theorem [13], [16] to determine Γ_i, after some algebraic manipulations, produces

$$\Gamma_i = \frac{1}{2} \iint_{S_s} (\overline{E}_s \times \overline{h}_{ti}) \cdot \hat{n}_i\, dS. \tag{6}$$

In (6), $\overline{E}_s$ is the induced electric field across the slot, S_s is the entire slot opening on the ground plane, $\hat{n}_i$ is an outward normal vector, i.e., $\hat{n}_{1,2} = -\hat{z}$ and $\hat{n}_{3,4} = \hat{z}$, $\overline{h}_{ti}$ is the magnetic test field on the slot opening and is related to $\overline{h}_i$ as $\overline{h}_{t1} = \overline{h}_2$, $\overline{h}_{t2} = \overline{h}_1$, $\overline{h}_{t3} = \overline{h}_4$, and $\overline{h}_{t4} = \overline{h}_3$. In order for Γ_i to be accurate, the induced slot electric field should be chosen appropriately and the magnetic-field eigenvectors on the ground plane determined exactly.

The induced electric field $\overline{E}_s$ for the maximum voltage V_s across the slot can be written as

$$\overline{E}_s = V_s \overline{e}_s \tag{7}$$

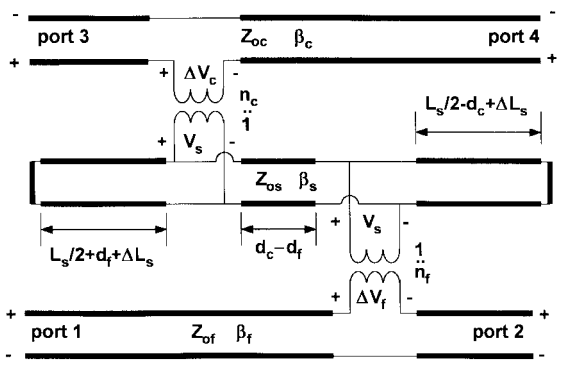

Fig. 2. Equivalent network model of the slot-coupled microstrip lines.

where $\overline{e}_s$ includes the effects of the slot-structure parameters and can be expressed in the following form for narrow slots:

$$\overline{e}_s = -\hat{x}' \frac{1}{\pi \sqrt{(W_s/2)^2 - x'^2}} g(y'). \tag{8}$$

In (8), $g(y')$ indicates the electric-field variation of the electrically short slot along its axis. Even though the piecewise-sinusoid (PWS) mode, when combined with the method of moments, yields good results [3], [8], an asymmetric cosine mode is chosen to represent $g(y')$ in this paper. A detailed expression for $g(y')$ is given in Section III.

III. Equivalent-Circuit Formulation

Slot-coupled microstrip lines can be viewed as microstrip-line discontinuities due to the slot on the ground plane. Thus, they can be represented by a simplified four-port network, shown in Fig. 2, which modifies the Das theory [5]. This equivalent circuit consists of two transmission lines for the microstrip feed and coupled lines, two ideal transformers, and three sections of slotline. Each of the outside ends of the two outer slotline sections is terminated by an extended slotline short. n_f and n_c denote the turn ratios of the ideal transformers. $Z_{\rm of}$ and $Z_{\rm oc}$ indicate the characteristic impedances of the microstrip lines. Z_s and β_s are the characteristic impedance and propagation constant of the slotline. ΔL_s is the extended slotline length due to the nonzero inductance at the end.

The voltage discontinuities ΔV_f and ΔV_c on the feed and coupled lines due to the presence of the slot are represented as

$$\Delta V_f = (\Gamma_1 - \Gamma_2) V_f \tag{9}$$

$$\Delta V_c = (\Gamma_3 - \Gamma_4) V_c \tag{10}$$

where V_f and V_c are the line voltages on the feed and coupled lines corresponding to the field eigenvectors. Due to the normalization in (5), the numerical figures of V_f and V_c are identical to those of $\sqrt{Z_{\rm of}}$ and $\sqrt{Z_{\rm oc}}$, respectively. Since n_f and n_c are defined as $\Delta V_f / V_s$ and $\Delta V_c / V_s$, respectively, they are expressed as

$$n_f = (\Gamma_1 - \Gamma_2) \sqrt{Z_{\rm of}} / V_s \tag{11}$$

$$n_c = (\Gamma_3 - \Gamma_4) \sqrt{Z_{\rm oc}} / V_s. \tag{12}$$

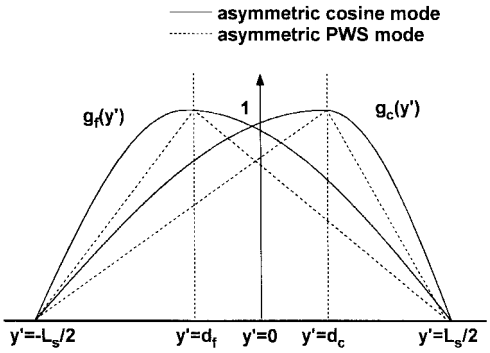

Fig. 3. Chosen electric-field distributions along the slot axis.

Substituting (6) into (11) and performing some vector operations produces the turn ratio n_f stated as

$$n_f = \frac{\sqrt{Z_{\rm of}}}{2}\left[(n_{\rm fx1} - n_{\rm fx2})\sin\theta_{\rm sf} + (n_{\rm fy1} + n_{\rm fy2})\cos\theta_{\rm sf}\right] \quad (13)$$

where $n_{\rm fx1}$ and $n_{\rm fy1}$ are

$$n_{\rm fx1} = \iint_{S_s} e_s h_{\rm fx} e^{-j\beta_f x}\, dS \quad (14)$$

$$n_{\rm fy1} = \iint_{S_s} e_s h_{\rm fy} e^{-j\beta_f x}\, dS. \quad (15)$$

In (14) and (15), $h_{\rm fx}$ and $h_{\rm fy}$ are the x- and y-components of $\overline{h}_f^+$. $n_{\rm fx2}$ and $n_{\rm fy2}$ take forms similar to (14) and (15) with the sign of β_f changed.

Using the finite Fourier transform relation of the magnetic-field components in (24) separates the integrals into x'- and y'-components. Then (14) and (15) can be expressed as

$$n_{\rm fx1} = \frac{1}{2L}\sum_{n=-\infty}^{\infty} \tilde{h}_{\rm fx}(k_{yn}, 0) I_{fx'1}(k_{yn}) I_{fy'1}(k_{yn}) \quad (16)$$

$$n_{\rm fy1} = \frac{1}{2L}\sum_{n=-\infty}^{\infty} \tilde{h}_{\rm fy}(k_{yn}, 0) I_{fx'1}(k_{yn}) I_{fy'1}(k_{yn}) \quad (17)$$

where $I_{fx'1}(k_{yn})$ and $I_{fy'1}(k_{yn})$ are

$$I_{fx'1}(k_{yn}) = J_0\left(\frac{W_s}{2}\left|k_{yn}\sin\theta_{\rm sf} - \beta_f\cos\theta_{\rm sf}\right|\right) \quad (18)$$

$$I_{fy'1}(k_{yn}) = \int_{-L_s/2}^{L_s/2} g(y') e^{-jb_{\rm fn1}(y'-d_f)}\, dy' \quad (19)$$

and

$$b_{\rm fn1} = k_{yn}\cos\theta_{\rm sf} + \beta_f \sin\theta_{\rm sf}. \quad (20)$$

The function $g(y')$ should contain the offset effect, which is at its maximum at the intersection of the slot and the microstrip line. For a structure with two intersections of different offset distances like the present one, it is difficult to describe the unique function of $g(y')$ analytically. Therefore, for the sake of simulation, $g(y')$ is chosen as $g_f(y')$ for the evaluation of n_f and as $g_c(y')$ for n_c, and are depicted in Fig. 3. The expression of $g_f(y')$ is given as

$$g_f(y') = \begin{cases} \cos p_f(y' - d_f), & \text{for } -(L_s/2) < y' < d_f \\ \cos q_f(y' - d_f), & \text{for } d_f < y' < (L_s/2) \end{cases} \quad (21)$$

where

$$p_f = \frac{\pi}{2(L_s/2 + d_f)} \quad q_f = \frac{\pi}{2(L_s/2 - d_f)}. \quad (22)$$

The expression of $g_c(y')$ is similar. Equation (19) can then be evaluated analytically, and is stated as

$$I_{fy'1}(k_{yn}) = \frac{p_f e^{jb_{\rm fn1}(L_s/2+d)} - jb_{\rm fn1}}{p_f^2 - b_{\rm fn1}^2} + \frac{q_f e^{-jb_{\rm fn1}(L_s/2-d)} + jb_{\rm fn1}}{q_f^2 - b_{\rm fn1}^2}. \quad (23)$$

Exactly the same procedure can be used to evaluate $n_{\rm fx2}$, $n_{\rm fy2}$, and n_c.

IV. Results and Discussions

To show the validity of the present theory, it is used to determine the turn ratios n_f and n_c. The slotline parameters Z_s, β_s, and ΔL_s can be calculated by using various analytical methods [17]. These values make it possible to compute the scattering parameters for the equivalent network. The results can then be compared with the measurements and computation data from previous theories and the rigorous solution.

First, the slot-coupled microstrip lines are treated with $d_f = d_c = 0$ mm and $\theta_{\rm sf} = \theta_{\rm sc} = 0°$. The structure parameters are $W_f = W_c = 2.54$ mm, $h_f = h_c = 0.762$ mm, $\epsilon_{\rm rf} = \epsilon_{\rm rc} = 2.22$, $L_s = 15$ mm, and $W_s = 1.1$ mm. The computed slotline parameters and turn ratios are shown in Fig. 4(a) and (b), where β_0 is the propagation constant for free space. Since the feed and coupled lines are the same, n_f is equal to n_c. The result for the turn ratios slightly increases with the frequency. For comparison, the turn ratios evaluated from the Das theory [5], which are larger than the present results and decrease as the frequency increases, are also included. Since the Das theory is based on the assumption that the matched slotline is infinite, the interaction between the electric field on that slotline and the magnetic field of the microstrip lines is larger than for the present finite slot. Using the present theory and the symmetry of the coupling structure reveals that the relation $S_{11} = S_{31} = -S_{41}$ holds. The computed results for the scattering parameters S_{11} and S_{21} are shown in Fig. 4(c) along with those measured and computed by Herscovici *et al.* [3] and computed by Das [5]. Herscovici *et al.* computed the scattering parameters by applying the method of moments based on the reciprocity theorem. Das obtained similar results from the equivalent circuit by using the turn ratio in Fig. 4(b) and fixing ΔL_s to 3 mm, independent of the frequency. However, ΔL_s, by nature, should change as the frequency varies. When the scattering parameters are calculated using the Das theory with ΔL_s obtained from the rigorous solution [17], as shown in Fig. 4(b), the results reveal some discrepancies with Herscovici *et al.*, as shown in Fig. 4(c). Therefore, Das' method to calculate the turn ratio

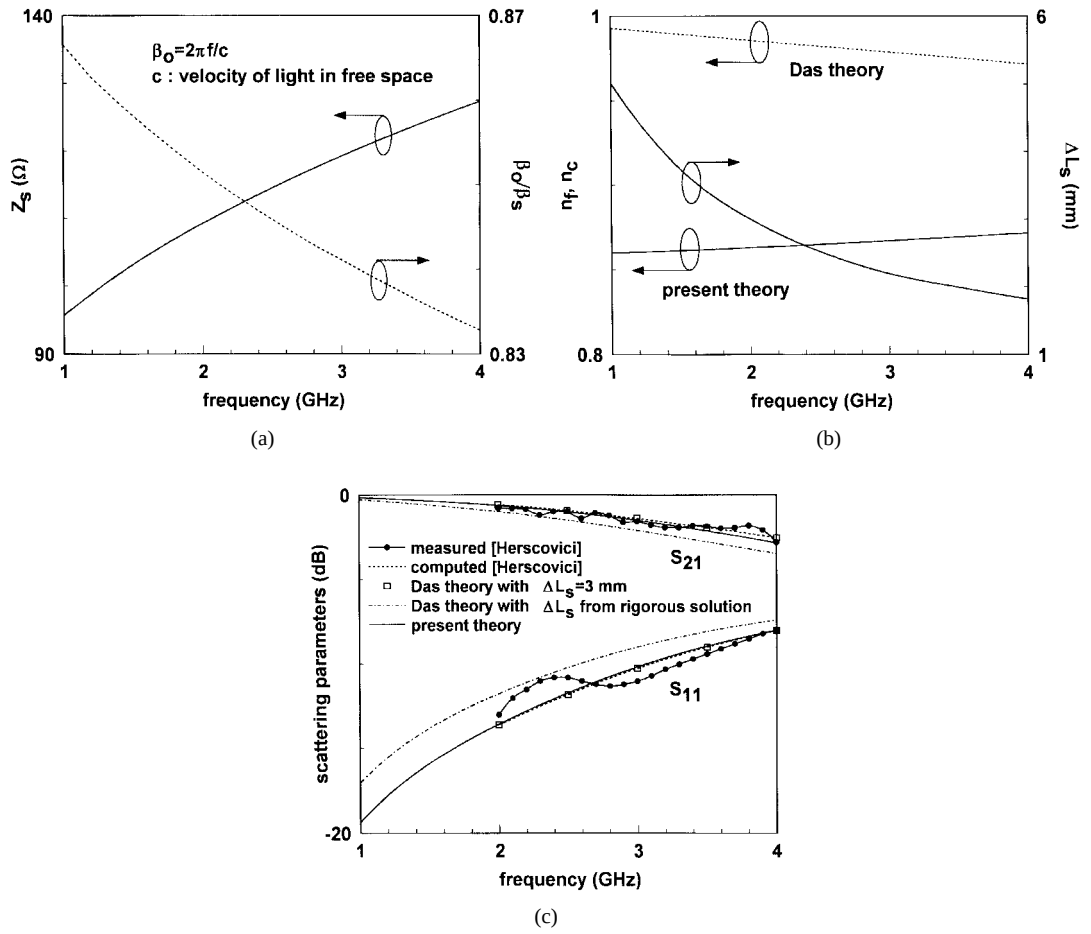

Fig. 4. Network and scattering parameters of the slot-coupled microstrip lines ($W_f = W_c = 2.54$ mm, $h_f = h_c = 0.762$ mm, $\epsilon_{\rm rf} = \epsilon_{\rm rc} = 2.22$, $L_s = 15$ mm, $W_s = 1.1$ mm, $d_f = d_c = 0$ mm, $\theta_{\rm sf} = \theta_{\rm sc} = 0^\circ$). (a) Propagation characteristics of the slotline. (b) Turn ratios and extended slotline length. (c) Scattering parameters.

needs to be modified when applied to a finite-length slot. In contrast, the present theory yields scattering parameters which highly agree with the conclusions of Herscovici *et al.* over the frequency range from 2 to 4 GHz, except for small ripples in the measured data. The ripples may have resulted from a fabrication error in the structure, such as an air gap between the two substrates or a minor discontinuity between connectors in the measurement process.

Secondly, the characteristics of slot-coupled microstrip lines are examined as the slot length varies. The structure parameters are $W_f = W_c = 4.3$ mm, $h_f = h_c = 1.588$ mm, $W_s = 1$ mm, $\epsilon_{\rm rf} = \epsilon_{\rm rc} = 2.54$, $d_f = d_c = 0$ mm, and $\theta_{\rm sf} = \theta_{\rm sc} = 0^\circ$. Fig. 5(a) shows the turn ratios calculated by the present and Das theories as the slot length varies from 2 to 12 mm at 3 GHz. The present method produces increasing turn ratios as the slot length increases because of more interaction between the slot electric field and the magnetic field of the microstrip lines, whereas the turn ratio in Das is constant. The slotline parameters at 3 GHz are $Z_s = 108.2\ \Omega$, $\beta_0/\beta_s = 0.742$, and $\Delta L_s = 2.026$ mm. The computed results of S_{31} are shown in Fig. 5(b), with the measured and computed data from Kumar [1], as well as the computed conclusion from Das. It is clear that the Das result does not agree with the measured one, and the discrepancy increases as the slot length decreases. It is also evident that the result computed by Kumar, which is based on the small-aperture coupling theory, gradually deviates more and more from the measured data as the slot length increases. However, the results of the present theory are consistent along the entire range of the slot length considered.

Next, the present theory is applied to slot-coupled microstrip lines with $\theta_{\rm sf} \neq 0^\circ$ and $\theta_{\rm sc} \neq 0^\circ$, as investigated by Ono *et al.* [7]. The structure parameters are the same as in the circuit considered for Fig. 4, except the slot inclination angles. Therefore, the slotline parameters in Fig. 4(a) and (b) can also be used. Fig. 6(a) shows the calculated turn ratios as the inclination angles vary at 2 GHz. The turn ratios decrease as the inclination angles increase. Fig. 6(b) depicts the results of S_{41} for two different slot inclination angles and compares them with the measured and computed results reported by Ono *et al.* over the frequency range from 1 to 3 GHz. Again, the result shows a good agreement.

For the fourth example, the proposed network model is applied to slot-coupled microstrip lines with $d_f \neq 0$, $d_c \neq 0$, and $\theta_{\rm sf} = \theta_{\rm sc} = 0^\circ$. The structure parameters considered are $W_f = W_c = 2.4$ mm, $h_f = h_c = 0.762$ mm, $\epsilon_{\rm rf} = \epsilon_{\rm rc} = 2.22$, $L_s = 14$ mm, and $W_s = 0.8$ mm [4]. Fig. 7(a) shows the turn ratios as a function of the offset distances calculated from two different distributions for the electric field along the slot. One

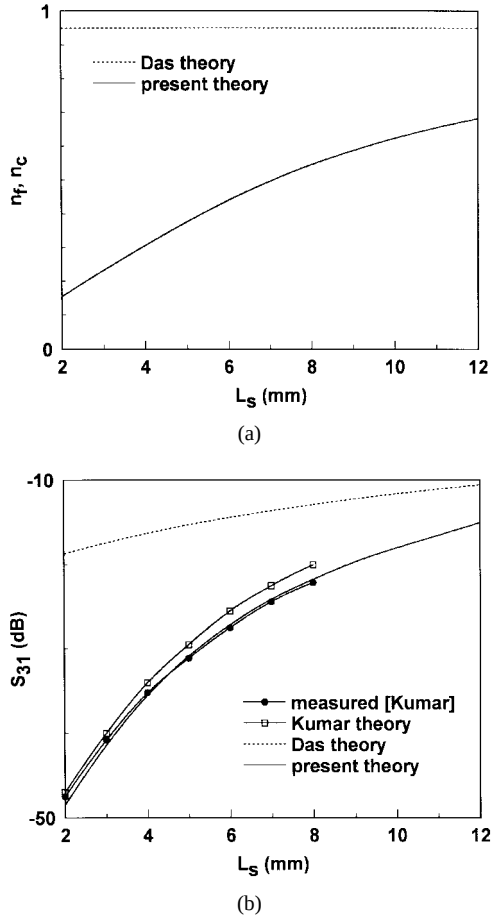

Fig. 5. Computed results of the slot-coupled microstrip lines for different slot lengths ($W_f = W_c = 4.3$ mm, $h_f = h_c = 1.588$ mm, $W_s = 1$ mm, $\epsilon_{\rm rf} = \epsilon_{\rm rc} = 2.54$, $d_f = d_c = 0$ mm, $\theta_{\rm sf} = \theta_{\rm sc} = 0^\circ$, $f = 3$ GHz). (a) Turn ratios. (b) Scattering parameter S_{31}.

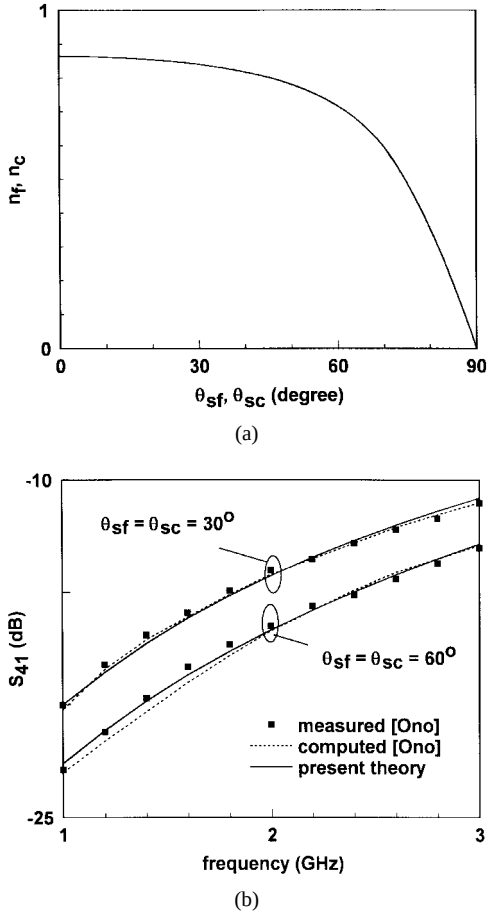

Fig. 6. Computed results of the slot-coupled microstrip lines for different inclination angles ($W_f = W_c = 2.54$ mm, $h_f = h_c = 0.762$ mm, $L_s = 15$ mm, $W_s = 1.1$ mm, $\epsilon_{\rm rf} = \epsilon_{\rm rc} = 2.22$, $d_f = d_c = 0$ mm). (a) Turn ratios at $f = 2$ GHz. (b) Scattering parameter S_{41}.

is an asymmetric cosine mode, and the other is an asymmetric PWS mode. Both modes yield decreasing turn ratios as the offset distances increase, and the turn ratios for the cosine mode are larger than those for the PWS mode. Fig. 7(b) shows the results for S_{31} at 2 GHz as a function of d_c when d_f is fixed at -1 mm. The slotline parameters in the present theory are $Z_s = 101.8\ \Omega$, $\beta_0/\beta_s = 0.837$, and $\Delta L_s = 2.699$ mm. Note that the asymmetric cosine-mode distribution agrees much closer with the rigorous solution of Wakabayashi *et al.* [4] than the asymmetric PWS mode distribution.

The fifth example treats a general case where $d_f = -1$ mm, $d_c = 2$ mm, $\theta_{\rm sf} = 30^\circ$, and $\theta_{\rm sc} = 60^\circ$. The structure parameters of the circuit are the same as those in Fig. 4, except the offset distances and inclination angles. The turn ratios calculated by the present theory are shown in Fig. 8(a). The computed scattering parameters highly agree with the results computed by the method of moments,[1] as shown in Fig. 8(b).

Finally, the present theory is applied to a practical design problem posed by the slot-coupled, back-to-back microstrip/microstrip transition in Fig. 9. We fabricated the transition, and it consists of slot-coupled microstrip lines and proper matching networks. The geometry of the slot-coupled microstrip lines is the same as in Fig. 4. The circuit optimization for the microstrip matching networks[2] gives the following structure parameters: $L_{\rm ef} = L_{\rm ec} = 26.4$ mm, $L_{\rm qf} = L_{\rm qc} = 25.62$ mm, $W_{\rm qf} = W_{\rm qc} = 1.5$ mm, and $L_{\rm mf} = L_{\rm mc} = 17.95$ mm. The measured scattering parameters are plotted in Fig. 10, along with the results computed by the present theory over the frequency range from 1 to 3 GHz. It is clear that the two results agree.

V. Conclusions

This paper proposed a general theory to analyze slot-coupled microstrip lines with a view to developing an improved equivalent-network model, which can tolerate the effects of various structure parameters, including inclination angles and offset distances. The equivalent four-port network consists of two microstrip lines, two ideal transformers, and an extended slotline terminated with short circuits. The turn ratios of the transformers are explicitly formulated in terms of the induced electric field on the slot and magnetic fields of the microstrip lines by invoking the reciprocity theorem. For computational convenience and efficiency, a finite Fourier transform in conjunction with the spectral-domain immittance approach is used to evaluate the magnetic fields on the

[1] HP Momentum, Hewlett-Packard Company, Santa Rosa, CA.

[2] HP 85150B RF and Microwave Design Systems, Hewlett-Packard Company, Santa Rosa, CA.

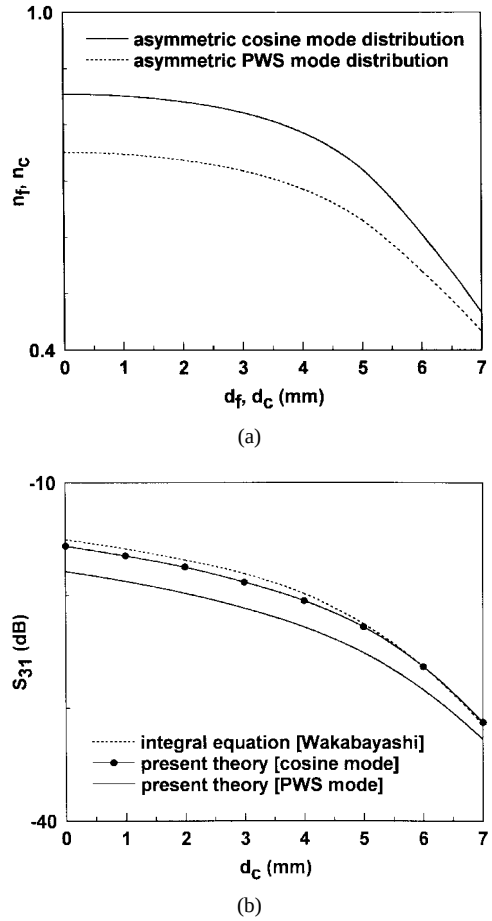

Fig. 7. Computed results of the slot-coupled microstrip lines for different offset distances ($W_f = W_c = 2.4$ mm, $h_f = h_c = 0.762$ mm, $L_s = 14$ mm, $W_s = 0.8$ mm, $\epsilon_{\rm rf} = \epsilon_{\rm rc} = 2.22$, $\theta_{\rm sf} = \theta_{\rm sc} = 0°$, $f = 2$ GHz). (a) Turn ratios. (b) Scattering parameter S_{31} for $d_f = -1$ mm.

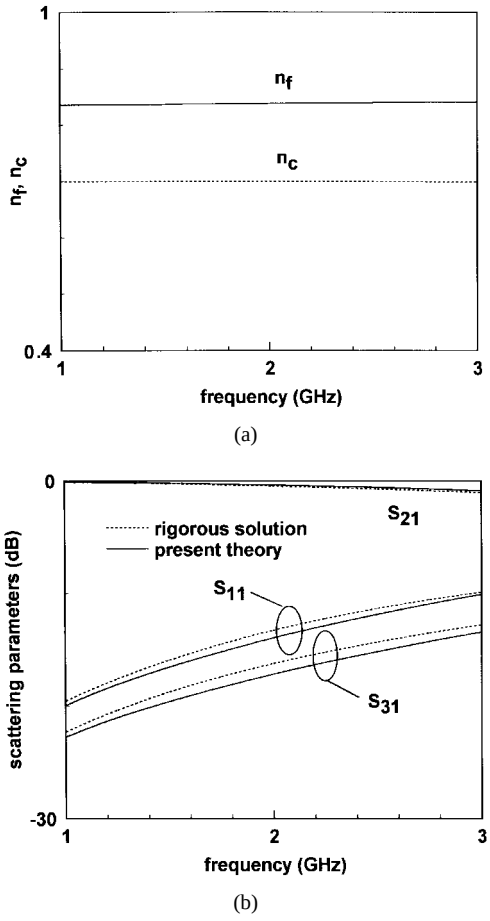

Fig. 8. Computed results of the slot-coupled microstrip lines for different offset distances and inclination angles ($W_f = W_c = 2.54$ mm, $h_f = h_c = 0.762$ mm, $L_s = 15$ mm, $W_s = 1.1$ mm, $\epsilon_{\rm rf} = \epsilon_{\rm rc} = 2.22$, $d_f = -1$ mm, $d_c = 2$ mm, $\theta_{\rm sf} = 30°$, $\theta_{\rm sc} = 60°$). (a) Turn ratios. (b) Scattering parameters.

ground plane of the microstrip lines. The scattering parameters are determined from the equivalent-network model using the general-network theory. The present theory was then applied to five different configurations of slot-coupled microstrip lines, which had been treated previously in the literature. A two-port practical fabrication of the transition was also completed. The measured scattering parameters and those computed by the present theory for the configuration showed a high agreement, which verified the theory's validity. Due to its simplicity and efficiency, the proposed network model is useful for analyzing and designing slot-coupled microstrip circuits. The present theory can also be extended to the analysis of slot-coupled multilayer microstrip circuits.

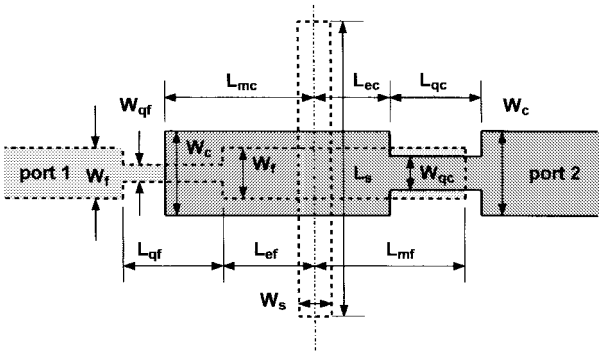

Fig. 9. A symmetrical, slot-coupled back-to-back microstrip/microstrip transition. For clarify, the widths of the coupled line are drawn larger than the feed line.

APPENDIX

The x- and y-components of the magnetic-field eigenvector for the feed line, $h_{\rm fx}$ and $h_{\rm fy}$ in (14) and (15), can be evaluated from the forward-traveling current, whose magnitude is $1/\sqrt{Z_{\rm of}}$. The microstrip line in Fig. 11 is assumed to be surrounded by fictitious boundary walls at a large distance $y = \pm L$ such that the electrically conducting walls do not disturb the electromagnetic-field distribution around the line. This situation enables use of the following finite Fourier transform along the y-direction instead of the infinite Fourier integral of $h_{\rm fx}$:

$$h_{\rm fx}(y,z) = \frac{1}{2L}\sum_{n=-\infty}^{\infty} \tilde{h}_{\rm fx}(k_{yn},z)e^{-jk_{yn}y} \tag{24}$$

$$\tilde{h}_{\rm fx}(k_{ym},z) = \int_{-L}^{L} h_{\rm fx}(y,z)e^{+jk_{yn}y}\,dy \tag{25}$$

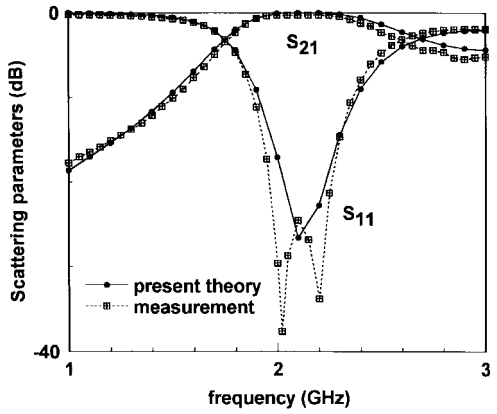

Fig. 10. Scattering parameters S_{11} and S_{21} of the microstrip/microstrip transition in Fig. 9 ($W_f = W_c = 2.54$ mm, $h_f = h_c = 0.762$ mm, $L_s = 15$ mm, $W_s = 1.1$ mm, $\epsilon_{\rm rf} = \epsilon_{\rm rc} = 2.22$, $d_f = d_c = 0$ mm, $\theta_{\rm sf} = \theta_{\rm sc} = 0^\circ$, $L_{\rm ef} = L_{\rm ec} = 26.4$ mm, $L_{\rm qf} = L_{\rm qc} = 25.62$ mm, $W_{\rm qf} = W_{\rm qc} = 1.5$ mm, $L_{\rm mf} = L_{\rm mc} = 17.95$ mm).

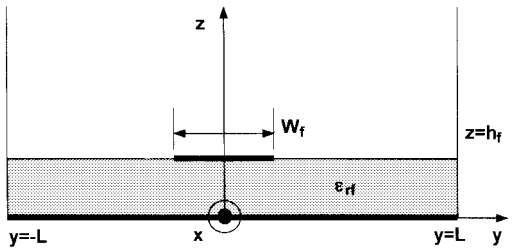

Fig. 11. Microstrip line with the fictitious walls of the perfect electric conductor at $y = \pm L$.

with

$$k_{yn} = \frac{n\pi}{L}, \qquad n = -\infty, \cdots, -1, 0, +1, \cdots, +\infty. \tag{26}$$

It is possible to define $h_{\rm fy}$ and its finite Fourier transform the same way.

Since the surface current density on the narrow strip is assumed to have only the x-component $J_{\rm fx}$

$$J_{\rm fx}(y) = \frac{1}{\sqrt{Z_{\rm of}}} \frac{1}{\pi\sqrt{(W_f/2)^2 - y^2}} \tag{27}$$

its Fourier transform $\tilde{J}_{\rm fx}$ becomes the first-kind Bessel function of zeroth order

$$\tilde{J}_{\rm fx}(k_{yn}) = \frac{1}{\sqrt{Z_{\rm of}}} J_0\left(\frac{W_f}{2}\,|k_{yn}|\right). \tag{28}$$

Using the spectral-domain immittance approach [14], the Fourier transforms of the magnetic-field components on the plane just below the interface of the substrate and air, which corresponds to $z = h_f^-$, can be derived as

$$\tilde{h}_{\rm fx}(k_{yn}, h_f^-) = \tilde{G}_{fxx}^{hJ} \tilde{J}_{\rm fx}(k_{yn}) \tag{29}$$

$$\tilde{h}_{\rm fy}(k_{yn}, h_f^-) = \tilde{G}_{fyx}^{hJ} \tilde{J}_{\rm fx}(k_{yn}) \tag{30}$$

where

$$\tilde{G}_{fxx}^{hJ} = \frac{\beta_f k_{yn}}{{\beta_f}^2 + k_{yn}^2} \left[\frac{-Y_{\rm TM}^-}{Y_{\rm TM}^- + Y_{\rm TM}^+} + \frac{Y_{\rm TE}^-}{Y_{\rm TE}^- + Y_{\rm TE}^+}\right] \tag{31}$$

$$\tilde{G}_{fyx}^{hJ} = \frac{1}{\beta_f^2 + k_{yn}^2} \cdot \left[\beta_f^2 \frac{Y_{\rm TM}^-}{Y_{\rm TM}^- + Y_{\rm TM}^+} + k_{yn}^2 \frac{Y_{\rm TE}^-}{Y_{\rm TE}^- + Y_{\rm TE}^+}\right]. \tag{32}$$

The parameter $Y_{\rm TM}^-$ in (31) and (32) is the input wave admittance for the $\rm TM_z$-mode looking downward from the plane $z = h_f$ [14]. The superscript $+$ denotes the input wave admittances looking upward from the same plane. The other admittance parameters are defined in a similar fashion. The Fourier transforms of the magnetic-field components on the ground plane can now be expressed as

$$\tilde{h}_{\rm fx}(k_{yn}, 0) = \frac{\tilde{h}_{\rm fx}(k_{yn}, h_f^-)}{\cosh(\gamma_{fzn} h_f)} \tag{33}$$

$$\tilde{h}_{\rm fy}(k_{yn}, 0) = \frac{\tilde{h}_{\rm fy}(k_{yn}, h_f^-)}{\cosh(\gamma_{fzn} h_f)} \tag{34}$$

with

$$\gamma_{fzn} = \sqrt{\beta_f^2 + k_{yn}^2 - k_o^2 \epsilon_{\rm rf}}. \tag{35}$$

Therefore, substituting (33) and (34) into (24) produces the required magnetic-field components on the ground plane.

REFERENCES

[1] M. Kumar, "Coupling between two microstrip lines through aperture," *Electron. Lett.*, vol. 14, no. 14, pp. 415–416, July 1978.
[2] T. Tanaka, K. Tsunoda, and M. Aikawa, "Slot-coupled directional couplers between double-sided substrate microstrip lines and their applications," *IEEE Trans. Microwave Theory Tech.*, vol. 36, pp. 1752–1757, Dec. 1988.
[3] N. Herscovici and D. M. Pozar, "Full-wave analysis of aperture-coupled microstrip lines," *IEEE Trans. Microwave Theory Tech.*, vol. 39, pp. 1108–1114, July 1991.
[4] T. Wakabayashi and T. Itoh, "Coupled displaced microstrip lines through a rectangular slot in a common ground plane," in *22nd European Microwave Conf. Dig.*, Helsinki, Finland, Aug. 1992, pp. 1165–1169.
[5] N. K. Das, "Generalized multiport reciprocity analysis of surface-to-surface transitions between multiple printed transmission lines," *IEEE Trans. Microwave Theory Tech.*, vol. 41, pp. 1164–1177, June/July 1993.
[6] A. M. Tran and T. Itoh, "Analysis of microstrip lines coupled through an arbitrarily shaped aperture in a thick common ground plane," in *IEEE MTT-S Int. Microwave Symp. Dig.*, Atlanta, GA, June 1993, pp. 819–822.
[7] K. Ono, Y. Sugasawa, H. Shiomi, T. Wakabayashi, S. Kawasaki, and Y. Mihara, "Characteristics of coupled microstrip lines through a rotated slot in a common ground plane," in *Proc. Symp. Progress Electromag. Res. (PIERS)*, Seattle, WA, July 1995, p. 996.
[8] Y. M. M. Antar, Z. Fan, and A. Ittipiboon, "Scattering parameters of arbitrarily oriented slot-coupled microstrip lines," *Proc. Inst. Elect. Eng.*, vol. 143, pp. 141–146, Apr. 1996.
[9] A. A. Omar and M. G. Stubbs, "Efficient full-wave solution of aperture coupling from microstrip to microstrip," in *ANTEM'94, Symp. Antenna Technol. Appl. Electromag.*, Ottawa, Ont., Canada, Aug. 1994, pp. 233–236.
[10] N. R. S. Simons, A. Sebak, and A. Ittipiboon, "Analysis of aperture-coupled microstrip antenna and circuit structures using the transmission line matrix method," *IEEE Antennas Propagat. Magazine*, vol. 37, pp. 27–37, Aug. 1995.

[11] A. Ittipiboon, D. Roscoe, and M. Cuhaci, "Analysis of slot-coupled double layer microstrip lines," in *ANTEM'90, Symp. Antenna Technol. Appl. Electromag.*, Winnipeg, Man., Canada, Aug. 1990, pp. 454–459.
[12] A. Ittipiboon, S. Meszaros, and M. Cuhaci, "S-parameter description of microstrip slot-couplers," in *ANTEM'92, Symp. Antenna Technol. Appl. Electromag.*, Winnipeg, Man., Canada, Aug. 1992, pp. 632–636.
[13] R. F. Harrington, *Time Harmonic Electromagnetic Fields*. New York: McGraw-Hill, 1961.
[14] T. Itoh, "Spectral domain immittance approach for dispersion characteristics of generalized printed transmission lines," *IEEE Trans. Microwave Theory Tech.*, vol. MTT-28, pp. 733–736, July 1980.
[15] R. E. Collin, *Foundations for Microwave Engineering*, 2nd ed. New York: McGraw-Hill, 1992.
[16] D. M. Pozar, "A reciprocity method of analysis for printed slot and slot-coupled microstrip antennas," *IEEE Trans. Antennas Propagat.*, vol. AP-34, pp. 1439–1446, Dec. 1986.
[17] K. C. Gupta, R. Garg, I. Bahl, and P. Bhartia, *Microstrip Lines and Slotlines*, 2nd ed.. Norwood, MA: Artech House, 1996.

Jeong Phill Kim (M'98) was born in Cheju, Korea, on November 2, 1964. He received the B.S. degree in electronic engineering from Seoul National University, Seoul, Korea, in 1988, and the M.S. and Ph.D. degrees in electrical engineering from Pohang University of Science and Technology, Pohang, Korea, in 1990 and 1998, respectively.

Since 1990, he has been with the Research and Development Center, LG Precision Co., Ltd., Yongin, Kyunggi-Do, Korea, where he has been involved in the design of various radar transmitters and receivers. His research interests include microstrip circuits and antennas, dielectric resonator antennas, numerical modeling and analysis, and microwave measurements.

Wee Sang Park (M'89) was born in Korea, in 1952. He received the B.S. degree in electronic engineering from Seoul National University, Seoul, Korea, in 1974, and the M.S. and Ph.D. degrees in electrical engineering from the University of Wisconsin at Madison, in 1982 and 1986, respectively.

From 1986 to 1988, he taught at Wichita State University, as a Visiting Assistant Professor. In 1988, he joined the Pohang University of Science and Technology (POSTECH), Pohang, Kyungbuk, Korea, where he is currently an Associate Professor in the Department of Electronic and Electrical Engineering. Since 1995, he has been Director of the Antenna Laboratory, Microwave Application Research Center, POSTECH. In 1997, he spent a one-year sabbatical leave in the Bioelectromagnetics Laboratory, University of Utah. He has been involved in the areas of electromagnetics, microwave and antenna engineering for the last 16 years. He has authored or co-authored over 80 technical journal articles and conference papers, and has made contributions to the developments of material-constant measurement methods using coaxial lines, cylindrical cavities, and dielectric resonators. He established network models for microstrip slots or slotlines for the design of microstrip patch and flared-notch antennas and multilayer microstrip circuit. He developed phase shifters with ferrite meander lines and p-i-n diodes; with these components, he developed microstrip phased-array antennas and tested them with a near-field probe. He also developed finite-difference time-domain (FDTD) codes to simulate the interaction between a cellular phone and the human head, and to analyze various microstrip discontinuities. His recent interest includes the measurement of the specific absorption rate (SAR) for portable phones and development of a bone-equivalent material for human phantoms. He is currently an Associate Editor of the Korea Electromagnetic Engineering Society.

Dr. Park is a member of the IEEE Microwave Theory and Techniques and IEEE Antennas and Propagation Societies, and the Institute of Electronics Engineers of Korea.